Applied Catalysis B: Environmental 126 (2012) 90–99

Contents lists available at SciVerse ScienceDirect

Applied Catalysis B: Environmental

journal homepage: www.elsevier.com/locate/apcatb

Photocatalytic degradation of imazalil in an aqueous suspension of TiO_2 and influence of alcohols on the degradation

R. Hazime[a,c], C. Ferronato[a], L. Fine[a], A. Salvador[b], F. Jaber[c], J.-M. Chovelon[a,*]

[a] Université de Lyon, Université Lyon 1, CNRS, UMR 5256, IRCELYON Institut de Recherches sur la Catalyse et l'Environnement de Lyon (IRCELYON), 2 avenue Albert Einstein, 69626 Villeurbanne Cedex, France
[b] Université de Lyon, Université Lyon 1, CNRS, UMR 5280, Laboratoire de sciences analytiques, 43 Boulevard du 11 novembre 1918, 69622 Villeurbanne Cedex, France
[c] Conseil National de la Recherche Scientifique, Commission Libanaise de l'Energie Atomique, Laboratoire d'Analyse de Pesticides et de Polluants Organiques, B.P. 11-8281, Riad El Solh, 1107 2260 Beyrouth, Lebanon

ARTICLE INFO

Article history:
Received 7 March 2012
Received in revised form 31 May 2012
Accepted 16 July 2012
Available online 22 July 2012

Keywords:
Imazalil degradation
Hydroxyl scavengers
Alcohols
Photocatalysis
HPLC–MS/MS

ABSTRACT

The photocatalytic degradation of imazalil, a probably carcinogen fungicide, was carried out in an aqueous suspension of titanium dioxide under UV irradiation. The influence of alcohols as hydroxyl scavengers (isopropanol, methanol) on the degradation was studied and different concentrations were used. We conclude that the degradation of imazalil occurs mainly by $OH^\bullet$ attack, since 80% of the degradation was inhibited in the presence of isopropanol [isopropanol] = 1000 [imazalil]. Using HPLC/DAD and LC–MS/MS analysis, nine intermediates were identified giving monohydroxylated, dihydroxylated and mostly a hole attack for other products. Their kinetic evolution profiles were plotted and compared to those with isopropanol. The quantity of photoproducts formed by $OH^\bullet$ radicals was decreased in the presence of isopropanol. After that a tentative pathway mechanism was proposed including mainly hydroxyl radical attack with the participation of holes in the degradation. Ion chromatography showed that nitrogen groups in imidazole were converted to both NH_4^+ and NO_3^-. In addition, TOC was examined in details and total mineralization was reached.

1. Introduction

The photocatalytic degradation of pesticides especially fungicides using TiO_2, is still attracting considerable attentions for applications to environmental problems [1,2]. The mechanism of this degradation has been intensively studied [3]. The role of active species leading to the initial photoreaction process has been deeply investigated, but it is still under active controversy [4]. The major uncertainty is whether oxidations proceed via direct electron transfer between substrate and positive holes, or via an $OH^\bullet$ radical mediated pathway [5]. To solve this controversy, inhibitors are used such as alcohols for hydroxyl radicals [5–14], iodide for both holes and hydroxyl radicals [10,15–17], para benzoquinone for superoxide [10], etc.

From available results, it can be suggested that the majority of organic substrates is oxidized by $OH^\bullet$ based on evidences including detection of hydroxylated products and spin trapping with subsequent ESR detection [18–21]. However direct hole oxidation could play a major role, such as carboxylic acids, that seemed to be oxidized primarily by valence band holes via a photo-kolbe process [22–24]. In addition, several authors have proved that holes could play a major role in the degradation of molecules. For example, in the case of acid orange 7, Chen et al. [5] have found that by using alcohols (isopropanol and methanol), the degradation were not significantly affected but were notably affected in the presence of iodide ion indicating that the degradation was mostly initiated by direct electron transfer reaction between a positive hole and a surface-bound AO7 molecule. Palominos et al. [10] have also obtained the same conclusion in the degradation of flumequine by using iodide ion and isopropanol.

In the present work, two different alcohols, isopropanol (i-PrOH) and methanol (MeOH)) having different rate constant $k_{(OH^\bullet,alcohol)}$ were used, to assess the role of $OH^\bullet$ in the degradation, and imazalil was chosen as the target for degradation. Imazalil is a systemic imidazole fungicide used to control a wide range of fungi on fruit, vegetables and ornamentals including powdery mildew on cucumber and black spot on roses. It is also used as a seed dressing and for post-harvest treatment of citrus, banana and other fruits to control storage decay. Under natural conditions, imazalil treatment will lead to resistant strains of fungi less likely than as a result of treatment with other fungicides [25].

* Corresponding author. Tel.: +33 4 72 43 26 38; fax: +33 4 72 44 81 14.
E-mail addresses: roumaysa_hazimeh@live.com (R. Hazime), corinne.ferronato@ircelyon.univ-lyon1.fr (C. Ferronato), Ludovic.fine@ircelyon.univ-lyon1.fr (L. Fine), arnaud.salvador@univ-lyon1.fr (A. Salvador), fjaber@cnrs.edu.lb (F. Jaber), jean-marc.chovelon@ircelyon.univ-lyon1.fr, chovelon@univ-lyon1.fr (J.-M. Chovelon).

0926-3373/$ – see front matter © 2012 Elsevier B.V. All rights reserved.
http://dx.doi.org/10.1016/j.apcatb.2012.07.007

Unfortunately, imazalil is cited as a probable carcinogen, by the Environmental Protection Agency U.S EPA. Imazalil is highly persistent in the soil environment, with a reported field half-life ranging from 120 to 190 days. A representative value is estimated to be 150 days for most soils and it is also moderately soluble in water [26]. As a consequence, it is important to use treatment methods for the removal of this pollutant from water.

At present, no studies on the removal of imazalil have been reported and a detailed study of the photocatalytic degradation might provide useful information for the use of TiO_2 in the treatment of imazalil in aqueous solution. Thus, the objectives of the study were (a) to evaluate the kinetics aspects of the process (adsorption, degradation rate, photolysis) (b) the identification of the reaction intermediates and their kinetic evolution profiles during the process of imazalil photodegradation to understand the mechanistic details of the photodegradation in the UV/TiO_2 light process, (c) monitoring the total organic carbon (TOC) and inorganic ions in the solution and (d) to assess the role of alcohols as hydroxyl scavenger during the degradation of imazalil and to compare the photoproducts without and with i-PrOH.

2. Materials and methods

2.1. Chemicals

Imazalil, (*RS*)-1-[2-(allyloxy)-2-(2,4-dichlorophenyl)ethyl]-1H-imidazole (99% purity) was purchased from Sigma–Aldrich and used as received. Titanium dioxide Degussa P25 was provided by Degussa (Frankfurt, Germany) with a specific BET area of 50 $m^2\ g^{-1}$ and a mean particle size of 30 nm. Polyvinylidene fluoride PVDF filters (0.45 μm) were purchased from Millipore. Acetonitrile (quality HPLC grade and LC–MS/MS grade), methanol, isopropanol, potassium iodide and formic acid (MS grade, 99% purity) were purchased from Aldrich. Water was obtained from a Millipore Waters Milli-Q water purification system. Other reagents were at least of analytical grade.

2.2. Photoreactor and light source

The irradiation was carried out in an open borosilicate (Pyrex) glass cell (cut-off at 295 nm, 4 cm diameter, 9 cm height) equipped with a magnetic stirring bar and water circulating jacket. The light source was a HPK 125 W Philips mercury lamp with main emission wavelength at 365 nm, cooled with a water circulation. The radiant flux entering the irradiation cell was measured by a VLX-3 W radiometer with a CX-365 detector (UV-A). A value of 31 mW cm^{-2} was found. For all experiences, before and during irradiation, the suspensions were magnetically stirred and the concentration of TiO_2 was optimized at 2.5 g L^{-1}.

2.3. Photocatalytic degradation procedure

Solutions of imazalil (25 mg L^{-1}) were prepared using Millipore Milli-Q deionized water and stored at 4 °C in the dark. The required pH (3, 6.5 and 10) was adjusted by adding diluted aqueous solution of phosphoric acid and NaOH. A 25 mL of imazalil solution and the required amount of TiO_2 powder (2.5 g L^{-1}) were then taken into the photoreactor. Before irradiation was turned on, the suspension was stirred for 30 min in the dark to reach the adsorption–desorption quasi-equilibrum. One first sample was taken out at the end of the dark adsorption period just before turning on the irradiation, in order to determine the bulk imazalil concentration. This value was taken as the initial concentration for the photocatalytic experiment, denoted hereafter as C_{eq} (in addition to C_0, the initial bulk concentration of pesticide before dark adsorption). During irradiation, samples were with-drawn regularly from the reactor and filtered immediately through 0.45 μm PVDF membrane filters to remove TiO_2 particles.

During the photocatalytic degradation of imazalil, the pH was measured and only a slight decrease was observed. In the case of use of alcohols (i-PrOH or MeOH), same procedure was used and the alcohol was added from the beginning of the experience, in the adsorption phase.

It should be noted that most of the measurements were repeated up to 3 times and the error for those repeated was less than 5%.

2.4. Chemical analysis

2.4.1. HPLC/DAD

The kinetic profile of imazalil during irradiation was monitored using Shimadzu VP series HPLC system consisting of LC-10AT binary pump, a SPD-M10A DAD and Schimadzu Class-VP software version (5.0). A 20 μL of filtered irradiated samples (25 mg L^{-1}) was directly injected. Analytical separation was performed using a column KROMASIL C4 (250 mm × 4.6 mm, particle size 5 μm) mobile phase, 70:30 (v/v) Acetonitrile/Water and flow rate of 1 mL min^{-1}. The detection wavelength was 202 nm.

2.4.2. LC/MS/MS

The separation, evolution and identification of intermediates formed during the photocatalytic degradation of imazalil solutions were performed by using LC–MS/MS analysis with a system comprising an HP 1100 series HPLC comprising binary pump and autosampler (Agilent Technologies, Waldbronn, Germany) coupled to a API4000 Q trap mass spectrometer (Applied Biosystems/MDS Analytical Technologies, Foster City, CA, USA) and equipped with a Turbo IonSpray source. Instrument control, data acquisition and processing were performed using the associated Analyst 1.5.1 software. The LC separation of the 20 μL injected sample was carried out on a Symmetry C_{18} column (100 mm × 2.1 mm, particle size 3.5 μm) from Waters (Milford, MA, USA). Elution was performed at a flow rate of 0.3 mL min^{-1} with water containing 0.1% (v/v) formic acid as eluent A and acetonitrile containing 0.1% (v/v) formic acid as eluent B, employing a linear gradient from 95% B to 60% B in 30 min. Then, column re-equilibration was performed for 10 min.

The injection duty cycle was 40 min, taking into account the column equilibration time. The mass spectrometer was initially tuned and calibrated using polypropylene glycol, reserpine and Agilent Tuning Mix (all Applied Biosystems, Foster City, CA, USA) according to the manufacturer's instructions. Q1 and Q3 were adjusted to 0.7 ± 0.1 a.m.u. FWHM for Full Scan, Product Ion scan and single ion monitoring mode, referred to as unit resolution. MS analysis was carried out in positive ionization mode using an ion spray voltage of 5500 V. The nebulizer (air) and the curtain gas flows (nitrogen) were set at 30 and 50 psi respectively. The Ion Spray source was operated at 450 °C with the auxiliary gas flow (air) set at 10 psi.

First full scan in positive and negative mode (m/z range 50–500, scan time, declustering potential ±30 V) was performed in order to identify the intermediates. Then, product ion scan MS/MS mode (declustering potential ±30 V, collision energy 20 eV, precursor ion m/z: 297, 255 and 159) was used for structure elucidation of the main degradation product. As positive ionization mode gave best sensitivity, this polarity ionization mode was retained for reaction kinetic photodegradation determination in single ion monitoring (SIM) (declustering potential 30 V).

For the HPLC–MS/MS kinetic studies of imazalil photodegradation, aliquots of the reaction mixture were taken at the beginning of the experiment and at regular time intervals during irradiation and after filtration to separate the TiO_2 particles.

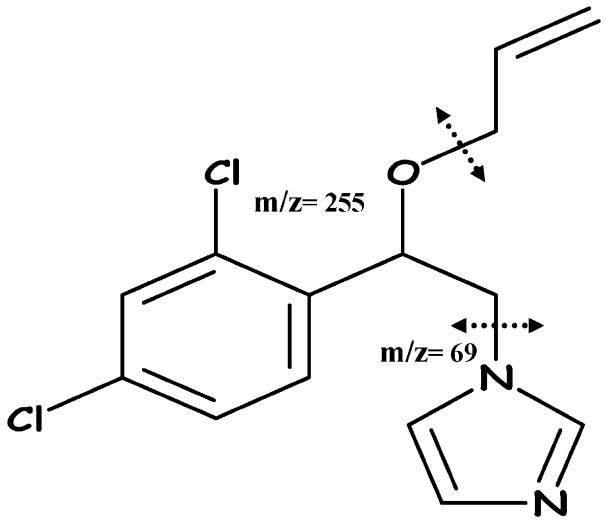

Fig. 1. Stucture of imazalil.

2.4.3. Ion chromatography

A Metrohm P224 instrument equipped with an autosampler and a conductimeter detector was employed. For cations analysis (ammoniums), a Metrohm Metrosep C4 column (150 mm × 4 mm) with a mobile phase made up of 1.7 mmol L^{-1} nitric acid and 0.7 mmol L^{-1} dipicolinic acid as eluent at a flow rate of 0.9 mL min^{-1} was used. The analysis of anions was performed by using a Metrosep A supp 5 column (150 mm × 4 mm) with 3.2 mM Na_2CO_3 and 1 mM $NaHCO_3$ as eluent at a flow of 0.7 mL min^{-1} (Fig. 1).

2.4.4. Total organic carbon analysis

In order to determine the extent of mineralization, total organic carbon (TOC) measurements were performed on filtered suspensions samples using TOCv-TN analyzer Schimadzu equipped with a Schimadzu ASI-V auto sampler device. 1 mL sample was mixed with 5% HCl solution (2 N) by purging out air for 90 s. Each sample was detected twice and a final TOC value was determined by calculating the average over the two measurements. Calibration was achieved by injecting standards of succinic acid solution.

3. Results and discussions

3.1. Adsorption of imazalil

In the dark with TiO_2 (Fig. 2, curve B), a slight decrease of imazalil was observed (5%) after 30 min of continuous stirring due to an adsorption of the pesticide on TiO_2 surface.

On the other hand, the complete disappearance of 84 μmol L^{-1} solution of imazalil was reached within 35 min in the presence of light (Fig. 2, curve C). Several experimental studies have indicated that the photocatalytical degradation rates of pesticides over illuminated TiO_2 could be interpreted by the Langmuir–Hinshelwood (L–H) kinetic model [27–30] but we are aware that the present kinetic data are not sufficient to conclude that the L–H mechanism is the most suitable model to describe the photocatalytic process of imazalil.

As it is seen in the inset in Fig. 2, the logarithm of the ratio of the initial concentration (C_0) to the concentration at a given time (C) versus time (t) is plotted. Imazalil degradation seems to follow a pseudo-first-order kinetic. The value obtained for k_{obs} determined by calculating the slope of the line was 0.11 min^{-1}.

3.2. Photolysis and photocatalysis of imazalil

In order to evaluate and to compare the efficiency of the photocatalytic process with that of direct photolysis, preliminary experiments were carried out at the same concentration of imazalil (C_0 = 84 μmol L^{-1} equivalent approximately to 25 mg L^{-1}) and at pH 6.5. Fig. 2 illustrates the kinetic evolution of imazalil concentration (μmol L^{-1}) under the following conditions: (A) irradiation without TiO_2 (photolysis), and (C) irradiation with TiO_2 (photocatalysis). As we can see, after 90 min of direct photolysis only 3% of imazalil degradation occurs (Fig. 2, curve A) which allows us to conclude that photolysis is negligible with respect to photocatalysis (curve C) and that experiments will occur in pure photocatalytic regime.

Additional experiments at pH 3 and 10 were conducted in order to study the effect of pH on the degradation. The lowest degradation was obtained for acidic pH, k = 0.07 min^{-1} whereas for alkaline pH, the degradation was the faster with k = 0.13 min^{-1}. This difference could be due to adsorption of imazalil (pK_a = 6.5) [31] onto TiO_2

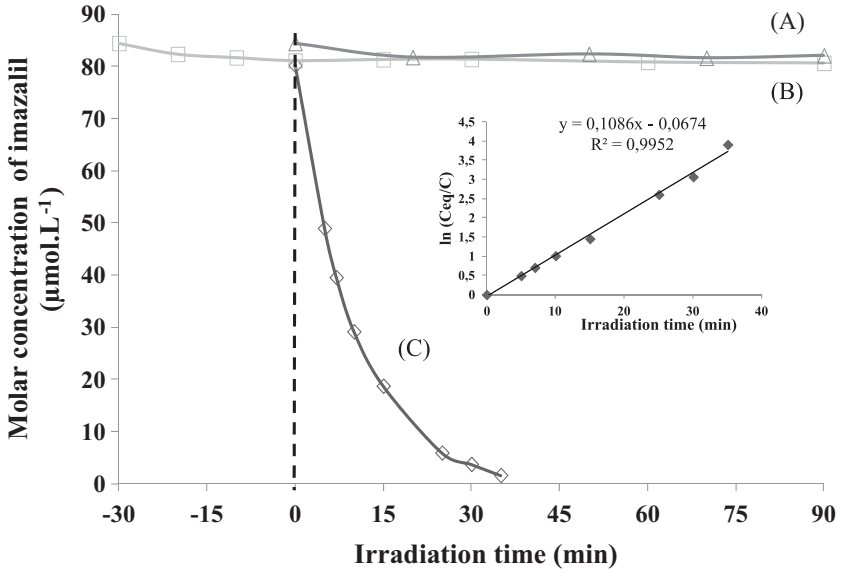

Fig. 2. Direct photolysis (A), adsorption (B) and imazalil degradation (C) (84 μmol L^{-1}). The inset shows the linear transform of the integrated first-order kinetics.

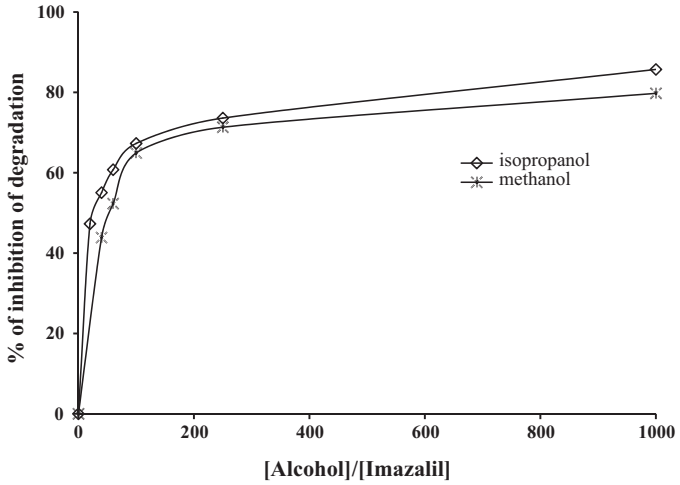

Fig. 3. Inhibition of degradation of imazalil in the presence of alcohols (methanol and isopropanol).

surface which depends on the pH. According to these equations, the surface of TiO_2 could have positive or negative charges:

$$pH < pH_{pzc}: \quad Ti{-}OH + H^+ \rightarrow TiOH_2{}^+ \tag{1}$$

$$pH > pH_{pzc}: \quad Ti{-}OH + OH^- \rightarrow TiO^- + H_2O \tag{2}$$

Since the pK_a of imazalil is 6.5, its adsorption at acidic pH is disfavored because of the electrostatic repulsion between the TiO_2 surface and imazalil. So by taking into account the Langmuir–Hinshelwood model, it should involve a decrease in the rate of the degradation. In addition, at alkaline pH, the enhancement of the degradation is due to a higher hydroxyl radicals amounts.

$$OH^- + h^+ \rightarrow OH^\bullet \tag{3}$$

3.3. Scavengers of hydroxyl radicals

3.3.1. Effect of methanol and isopropanol

The effect of alcohols, such as MeOH and i-PrOH, on the photocatalytic efficiency has commonly been used to better understand the mechanism of the degradation [5,7,10]. Though direct oxidation of short aliphatic alcohols by photogenerated holes probably happens, it can be considered as negligible because of their very weak adsorption on TiO_2 surface. So alcohols are usually used as diagnostic tools of $OH^\bullet$ radicals mediated mechanism. The oxidation potential of MeOH and its rate constant with $OH^\bullet$ are 0.55 V (versus NHE) [32] and $1.10^9\ M^{-1}\ s^{-1}$ respectively [13] while values for i-Pr-OH are −0.244 V [33] and $1.9.10^9\ M^1\ s^{-1}$[13].

Adsorption measurements demonstrated that MeOH had negligible influence on the adsorption amount of imazalil so that MeOH cannot compete for the adsorption sites with imazalil. Due to its low affinity to the TiO_2 surface, MeOH was expected to compete mainly with $OH^\bullet$ radicals [34,35]. If $OH^\bullet$ radicals dominated the photocatalytic oxidation of imazalil, the addition of MeOH would inhibit the reaction strongly. The effect of MeOH on the photodegradation of imazalil is shown in Fig. 3. It was found that MeOH has a remarkable influence on the photodegradation of imazalil as an increase of the MeOH concentration leads to an increase in the inhibition percent up to a steady value of 78% at the highest ratio [MeOH/imazalil] = 1000. The results suggested that $OH^\bullet$ radicals play a major role in the degradation. It is noteworthy that the use of several [alcohol]/[imazalil] ratio allowed us to determine the optimal value for the inhibition.

To confirm this finding, i-PrOH was also used, and Fig. 3 showed that the same conclusion can be drawn except the fact that inhibition with the latter is slightly higher. This difference could be related to the fact that the rate constant between $OH^\bullet$ and alcohol is higher in the case of i-PrOH.

Additional experiments using KI as hole and hydroxyl radical scavengers were performed (ratio [inhibitor]/[imazalil] = 100) and 90% of inhibition was found which is in line with the fact that hydroxyl radicals are mostly responsible of the degradation.

3.4. Degradation kinetics

3.4.1. Identification of photoproducts:

In order to characterize as many as possible the organic intermediates, a mixture of imazalil ($25\ mg\ L^{-1}$) solutions irradiated during four different time viz. 25, 45, 60 and 120 min was filtered and then analysed directly by HPLC–MS/MS. Blank analysis helped us to discard those peaks coming from the sample handling procedure and chromatographic system. First, molecular weights of photoproducts were determined by full scan analysis in negative and/or positive ion spray acquisition mode and then a MS analysis of the major compounds were performed in order to obtain structural information of each photoproduct. Nine major photoproducts were then detected and subsequently identified by interpretation of their MS spectra.

Table 1.

As can be seen, products from the first generation such as compounds **2**–**4** are identified as being monohydroxylated compounds. In order to determine the position of $OH^\bullet$ addition (aromatic or double bond), imazalil mass fragmentation spectra were firstly compared to the photoproducts masses observed during product ion scan analysis. Compound **4** exhibited the same molecular fragment than imazalil ($m/z = 255$), which corresponds to the absence of hydroxyl radical on the aromatic ring which leads to the conclusion that hydroxyl attack occurs on the double bond. On the other hand, compounds **2-3** for which $m/z = 271$ (255 + 16) correspond to the addition of hydroxyl radical on the aromatic ring.

Compound **5** was identified as a product coming from the reaction of hydroxyl radical with the ether function [36].

Compounds of second generation **6** and **7** were identified as dihydroxylated products with both hydroxyls on the double bond for compound **6** and both hydroxyls on benzene ring for compound **7**. In order to correctly characterize these compounds (position of hydroxylation), it would be necessary to isolate each of them from the degradation mixture and to perform its NMR analysis or to analyse them using an HPLC/^{1}H NMR methods [37] or more simply to determine the most probable positions attacked by hydroxyl radicals with theoretical calculations [38].

Compound **8** was identified as a fragmentation of imazalil in which a loss of $m/z = 41$ corresponding to $CH_2{-}CH{=}CH_2$ was identified. This compound still contain the imidazole ring due to the presence of ($m/z = 69$). Compound **9** $(M + H)^+ = 273$ was identified as compound **8** $(M + H)^+ = 257$ plus the addition of one hydroxyl radical. Compound **10** has odd molecular mass so it contains one atom of nitrogen and does not contain the imidazole ring ($m/z = 69$). No photoproduct either with one chlorine atom or without was detected in our analytical conditions which were not appropriate for these compounds.

3.4.2. Evolution of photoproducts and comparison of photoproducts without and with isopropanol

In order to better understand the reaction mechanisms involved in the photocatalytic degradation of imazalil, the evolution of the main intermediates (Fig. 4) was followed during the irradiation of a solution of imazalil ($25\ mg\ L^{-1}$). Thus, aliquots of the reaction

Table 1
Mass spectra data and structures of identified intermediates by LC–MS–MS after irradiation of imazalil solution in presence of TiO_2.

No.	Structure	Retention time (min)	$[M+H]^+$	Positive fragment
2	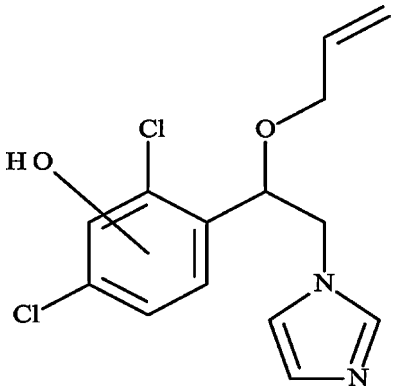	12.6	313	271, 215, 201, 69
3		15		
4	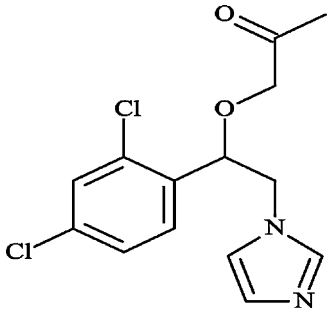	16.2	313	255, 215, 159, 69
5	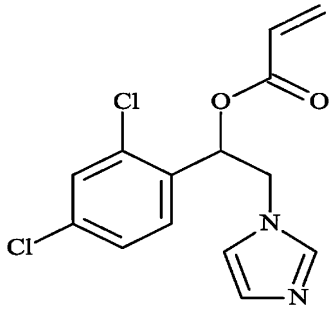	13.8	311	283, 239,159, 69
6	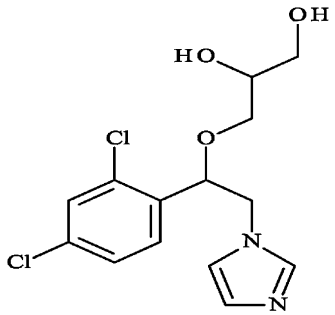	8.3	331	315, 239, 203, 69
7	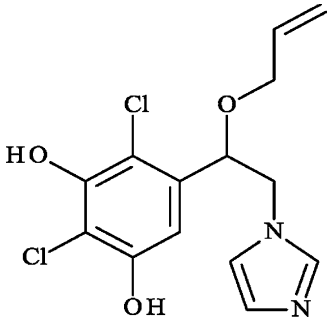	12.1	329	301, 261, 257, 69

Table 1 (*Continued*)

No.	Structure	Retention time (min)	$[M+H]^+$	Positive fragment
8	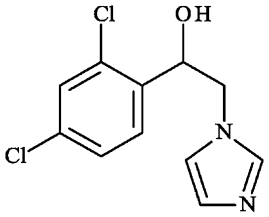	7.7	257	239, 189, 69
9	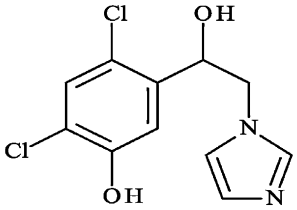	6.8	273	255, 205, 159, 69
10	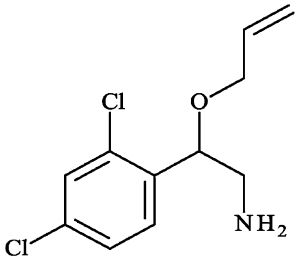	14.2	246	188, 153, 117

mixture were sampled at regular time intervals during photodegradation process up to 360 min and analyzed by HPLC–MS/MS. After 120 min of irradiation, no degradation products were detected.

To obtain complementary information on the photoproducts and the pathway of imazalil degradation, i-PrOH (hydroxyl scavenger) at the ratio [isoproponal/imazalil] = 1000 was added to ensure that inhibition is at its highest value. Fig. 5a–d shows the evolution of main photoproducts in the absence and in the presence of i-PrOH versus conversion rate of imazalil (%) (a and b) and versus irradiation time (c and d). From Fig. 5a and b, we can conclude that the same intermediates are obtained without and with i-PrOH but their respective quantities differ. For example, the quantity of products **2**, **3**, **4** and **6** were lower in presence of i-PrOH (hydroxyl radical scavenger) which allows us to conclude that they were generated by $OH^{\bullet}$ which is in line with the fact that they were proposed as being mono and di-hydroxylated intermediates. Product **5** decreases also in the presence of i-PrOH, certifying that its formation includes the attack by $OH^{\bullet}$, but its quantity remains higher than the quantity of monohydroxylated products.

On the other hand, products **8** and **10** were not influenced by the addition of i-PrOH, so that their formation could have implied other mechanism of degradation such as hole attack or other reactive radical attack.

From Fig. 5a and b, we can notice that for a given conversion rate, the whole detected photoproducts are less when isopropanol is used. So we have assumed that perhaps some of them were

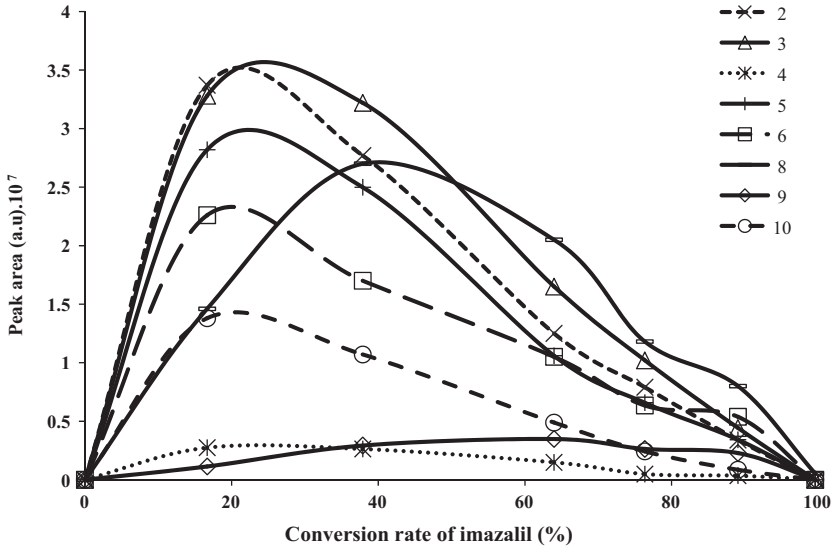

Fig. 4. Evolution of the quantity of main photoproducts versus the conversion rate of imazalil.

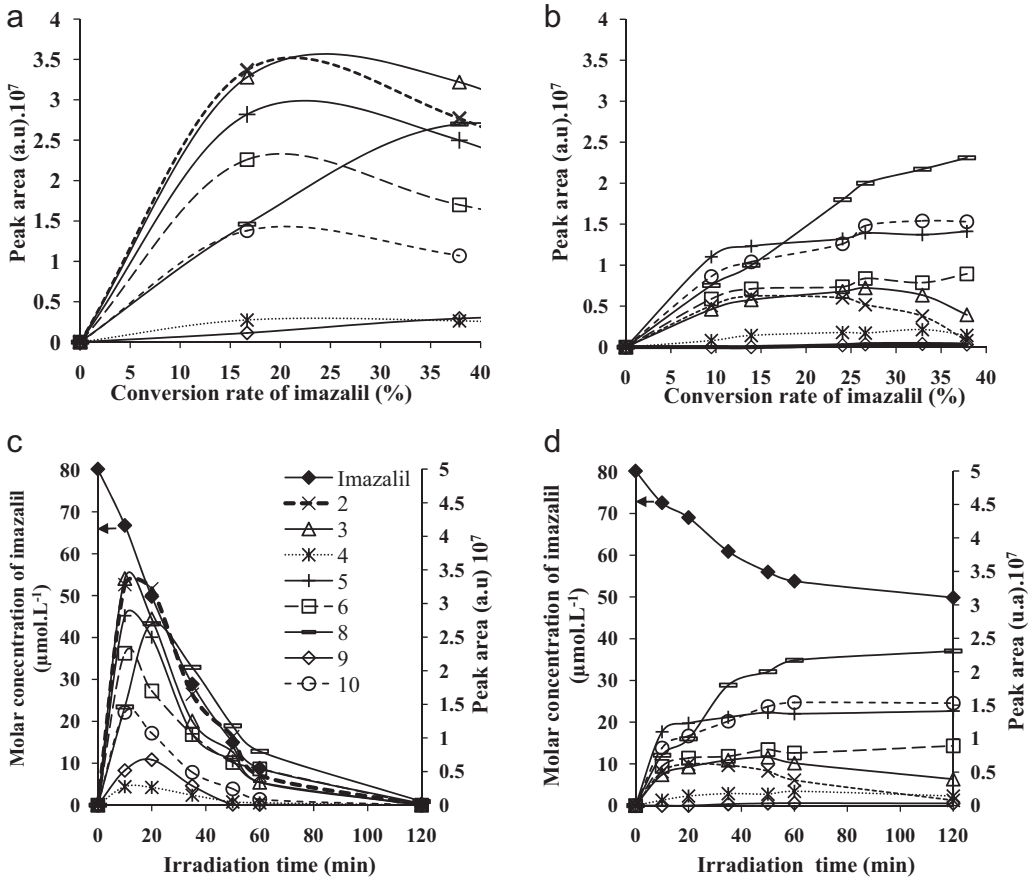

Fig. 5. Evolution of main photoproducts in the absence (a, c) and in the presence of isopropanol 84.4 μmol L^{-1} (b, d) versus conversion rate of imazalil (%) and versus irradiation time.

adsorbed on the TiO_2 surface and to confirm this hypothesis, extraction of the surface of TiO_2 using acetonitrile as solvent was performed. Indeed, results showed that a higher amount of imazalil on the surface was present with isopropanol than without but no significant photoproducts were found. A second hypothesis might be due to the presence of photoproducts not detected by our analytical method, such as the ones with one or without chlorine atoms.

Fig. 5d shows that after 120 min of imazalil degradation in presence of i-PrOH, its concentration reach a steady value which could be explained by the fact that imazalil and photoproducts accumulate since hydroxyl radicals are scavenged.

3.5. Degradation pathway

Based on the previous results, a possible photocatalytic degradation pathway of imazalil consisting of several steps was proposed in Fig. 6. As shown, all the intermediates are formed in mainly three different ways:

(i) Firstly, imazalil is attacked by $OH^{\bullet}$ radicals either on benzene ring or on double bond leading to three monohydroxylated products, which reach their maximum of concentrations after ca. 12 min of degradation and then decrease progressively to disappear from the solution after ca. 120 min, as shown in Fig. 4. Products **2** and **3** are obtained by hydroxylation of the benzene ring, whereas product **4** is obtained by hydroxylation of double bond as first step, then addition of oxygen, followed by a loss of $HO_2^{\bullet}$ and at the end transformation of alcohol to ketone function. Assuming that photoproducts **2**, **3** and **4** have a similar structure we can suggest that they have nearly the same response factor with respect to the MS analysis. In this case, by comparing the evolution profiles of these products it appears that **2** and **3** are concentrated and more rapidly formed than **4** (Fig. 5a) indicating a regioselective attack for $OH^{\bullet}$ radicals due to the highest electron density of the benzene carbon sites. In addition, we can even assume (even if HPLC–MS/MS analysis is unable to give us this data) that hydroxyl radicals attack occurs mainly on the carbon in ortho position with respect to chlorine atom (product **2** and **3**) since it is the most nucleophile position.

In addition, hydroxyl radical can lead to the abstraction of a hydrogen atom from the carbon in alpha position of the ether function [36,39,40] to give the formation of a ketone (product **5)** which reaches its maximum at ca.12 min.

(ii) Other intermediates result from the dihydroxylation of double bond and benzene ring to give compounds **6** and **7** respectively. Product **6** appears in the first minutes of the irradiation and its concentration increases up to reach a maximum at ca. 15 min. This product is able to yield product **4** by dehydration.

(iii) From the literature, compound **8** can be obtained by a hydroxyl attack on the ether function [32] but here since i-PrOH does not modify its concentration, we can suggest that another pathway of formation with hole attack or another reactive radical than $OH^{\bullet}$ could take place. Product **9** results from the addition of hydroxyl radical on product **8**. Product **10** was not influenced by the presence of i-PrOH so its formation could result from the opening of the imidazole ring by hole attack [41].

To resume all of these results, a tentative degradation pathway is suggested in Fig. 6.

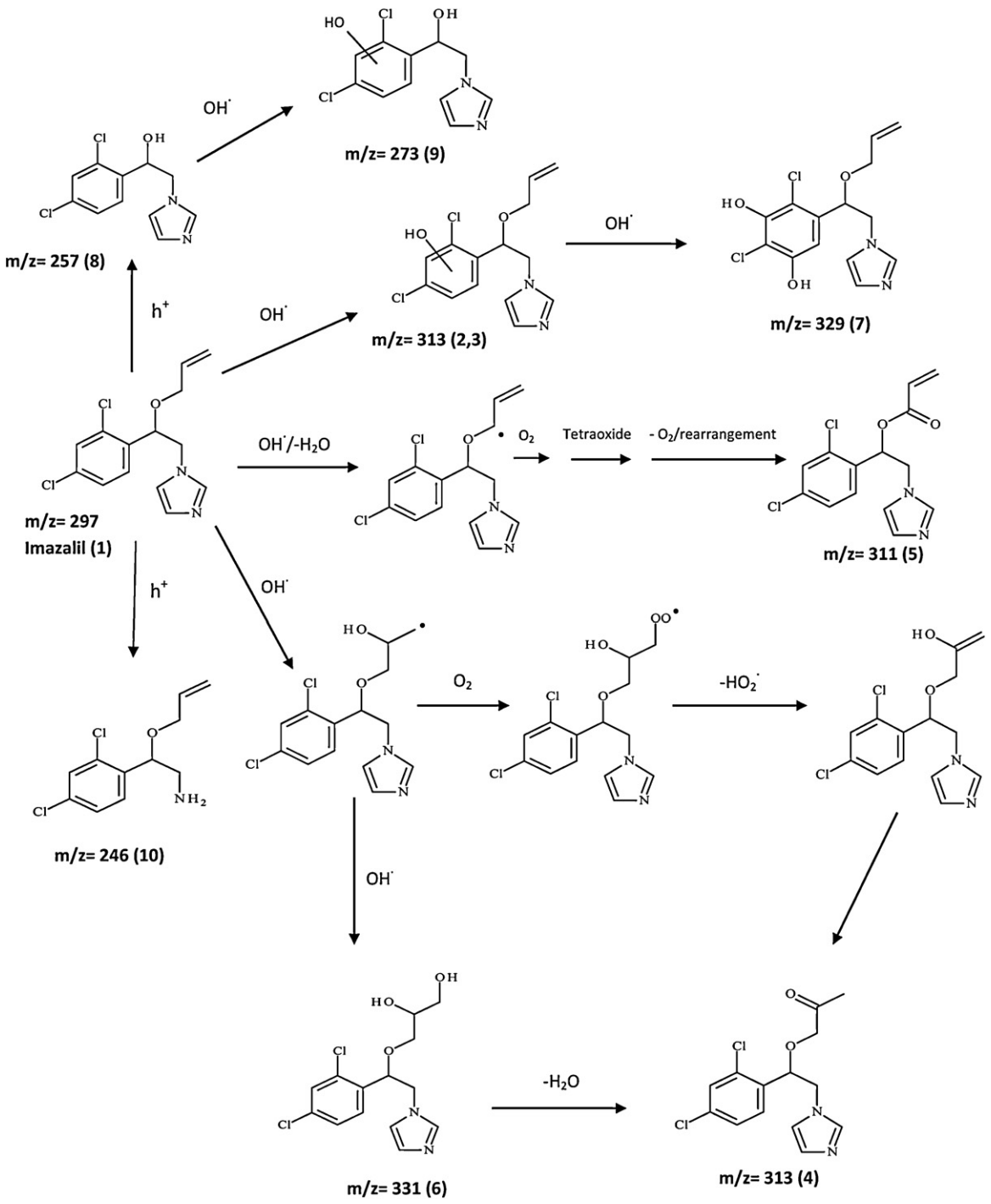

Fig. 6. Tentative degradation pathway of imazalil.

3.6. Evolution of mineralization

Complete mineralization is the ultimate step in water treatment process of organic molecules. It is thus important to follow not only the disappearance of the initial pollutant but also its mineralization into CO_2 and inorganic ions. Looking at the formula for imazalil (84 μmol L^{-1}), one can expect the formation of NO_3^- and/or NH_4^+ as well as Cl^-.

As can be seen Fig. 7, TOC removal followed a much slower rate compared to degradation of imazalil. The mineralization kinetic is rapid at the first 2 h of the treatment but becomes much slower at longer time because carboxylic acids formed by oxidative ring opening reactions are less reactive toward hydroxyl radicals compared to the aromatics. Thus, they are degraded more slowly than the initially introduced pesticide. Complete TOC removal was achieved after long irradiation time (around 800 min) to reach a constant number equal to 1, which corresponds to the measure of TOC for TiO_2 aqueous solution (background noise).

Regarding the inorganic ions, nitrogen in the imidazole was mineralized into ammonium (ca. 83 μmol L^{-1}) and nitrate (ca. 89 μmol L^{-1}) ions, which is confirmed by the mechanism proposed by Nohara et al. [41]. Ammonium ions were released faster than nitrate ions [42]. For chloride ions (ca. 168 μmol L^{-1}), they were all released after 120 min of irradiation.

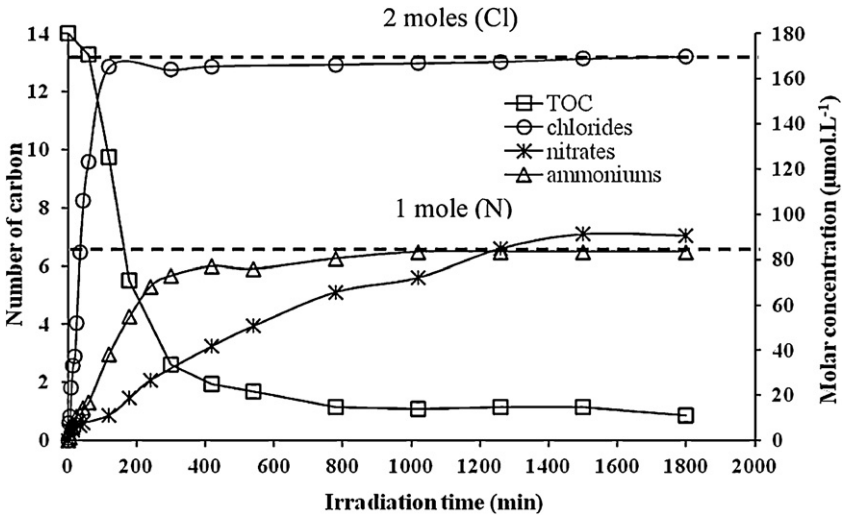

Fig. 7. Time course of TOC and inorganic ions (nitrates, ammoniums and chlorides) during imazalil photocatalytic degradation.

The overall equation, valid after long irradiation time in the presence of excess of oxygen, which describes the photocatalytic degradation of imazalil is presented below:

$$C_{14}H_{14}N_2OCl_2 + 17O_2 \rightarrow 14CO_2 + NH_4^+ + NO_3^- + 2H^+ + 2Cl^- + 4H_2O \quad (4)$$

4. Conclusions

Photodegradation using TiO_2 as a catalyst is an efficient method for degrading imazalil. A detailed study on its photocatalytic degradation was presented, from the kinetic process to the identification of byproducts, the investigation of reactional mechanism and influence of alcohols on the degradation.

The kinetic of imazalil follows a pseudo first order kinetic. Nine intermediates were identified and characterized through a mass spectra analysis using HPLC–MS/MS, giving insight into the early steps of the degradation process.

The presence of alcohols in the solution, inhibited the degradation of imazalil and the comparison of photoproducts without and with isopropanol showed that the quantity of some photoproducts resulting from hydroxyl attack were dramatically decreased in the presence of isopropanol and that hole attack or other reactive species is a complementary pathway in the degradation of imazalil.

The pathway proposed consists of hydroxylation of imazalil for the formation of most of the photoproducts (monohydroxylated and dihydroxylated) and mostly a hole attack for other products.

Complete mineralization was achieved, which was proved by the analysis of TOC and inorganic ions in solution.

Acknowledgements

The authors are thankful to the scientific services of IRCELYON, and to the LAPPO, CLEA, Liban.

References

[1] L. Lagunas-Allué, M.T. Martinez-Soria, J.S. Asensio, A. Salvador, C. Ferronato, J.M. Chovelon, Applied Catalysis B: Environmental 115/116 (2012) 285–293.
[2] D.A. Lambropoulou, I.K. Konstantinou, T.A. Albanis, A.R. Fernández-Alba, Chemosphere 83 (2011) 367–378.
[3] H.D. Burrows, M. Canle, J.A. Santaballa, S. Steenken, Journal of Photochemistry and Photobiology B 67 (2002) 71–108.
[4] D. Hufschmidt, L. Liu, V. Selzer, D. Bahnemann, Water Science and Technology 49 (2004) 135–140.
[5] Y. Chen, S. Yang, K. Wang, L. Lou, Journal of Photochemistry and Photobiology A: Chemistry 172 (2005) 47–54.
[6] C. Richard, F. Bosquet, J.-F. Pillichowski, Journal of Photochemistry and Photobiology A: Chemistry 108 (1997) 45–49.
[7] A.A. Khodja, T. Sehili, J-F. Pilichowski, P. Boule, Journal of Photochemistry and Photobiology A: Chemistry 141 (2001) 231–239.
[8] N. Daneshvar, D. Salari, A.R. Khataee, Journal of Photochemistry and Photobiology A: Chemistry 162 (2004) 317–322.
[9] C.-H. Yu, C.-H. Wu, T.-H. Ho, P.K.A. Hong, Chemical Engineering Journal 158 (2010) 578–583.
[10] R. Palominos, J. Freer, M.A. Mondaco, H.D. Mansilla, Journal of Photochemistry and Photobiology A: Chemistry 193 (2008) 139–145.
[11] D.V. Sojic, V.B. Andreluh, D.Z. Orcic, B.F. Abramovic, Journal of Hazardous Materials 169 (2008) 94–101.
[12] A. Zertal, D. Molnar-Gabor, M.A. Malouki, T. Sehili, P. Boule, Applied Catalysis B 49 (2004) 83–89.
[13] G.V. Buxton, C.L. Greenstock, W.P. Ross, Journal of Physical Chemistry 17 (1988) 513.
[14] T. Sehili, P. Boule, J. Lemaire, Journal of Photochemistry and Photobiology A: Chemistry 50 (1989) 103–116.
[15] K.-I. Ishibashi, A. Fujishima, T. Watanabc, K. Hashimoto, Journal of Photochemistry and Photobiology A: Chemistry 134 (2000) 139–142.
[16] J. Rabani, K. Yamashita, K. Ushida, J. Stark, A. Kira, Journal of Physical Chemistry B 102 (1998) 1689–1695.
[17] T.M. El-Morsi, W.R. Budakowski, A.S. Abd-El-Aziz, K.J. Friesen, Environmental Science and Technology 34 (2000) 1018–1022.
[18] M.A. Grela, M.E.J. Coronel, A.J. Colussi, Journal of Physical Chemistry 100 (1996) 16940–16946.
[19] L.Z. Sun, J.R. Bolton, Journal of Physical Chemistry 100 (1996) 4127–4133.
[20] P.F. Schwarz, N.J. Turro, S.H. Bossmann, A.M. Braun, A.-M.A.A. Wahab, H. Durr, Journal of Physical Chemistry B 101 (1997) 7127–7134.
[21] Y. Nosaka, S. Komori, K. Yawata, T. Hirakawa, A.Y. Nosaka, Physical Chemistry Chemical Physics 5 (2003) 4731.
[22] Y. Mao, C. Schœneich, K.-D. Asmus, Journal of Physical Chemistry 95 (1991) 10080–10089.
[23] R.B. Draper, M.A. Fox, Langmuir 6 (1990) 1396–1402.
[24] J. Peral, J. Casado, J. Domenech, Journal of Photochemistry and Photobiology A: Chemistry 44 (1988) 209–217.
[25] H.-C. Su, A.-Y. Lin, Journal Food and Drug Analysis 11 (2003) 296–301.
[26] R.D. Wauchope, T.M. Buttler, A.G. Hornsby, P.W.M. Augustijn Beckers, J.P. Burt, Reviews of Environment Contamination and Toxicology 123 (1992) 10–12.
[27] J.C. D'Oliveria, G. Al-Sayyed, P. Pichat, Environmental Science and Technology 24 (1990) 990–996.
[28] C.S. Rurchi, D.R. Ollis, Journal of Catalysis 122 (1990) 178–192.
[29] J.M. Herrmann, Topics in Catalysis 34 (2005) 49–65.
[30] L. Lagunas-Allué, M-T. Martínez-Soria, J. Sanz-Asensio, A. Salvador, C. Ferronato, J.-M. Chovelon, Applied Catalysis B: Environmental 98 (2010) 122–131.
[31] M.R. Siegel, A. Kerkenaar, A. Kaars Sijpesteijn, European Journal of Plant Pathology 83 (1977) 121–133.
[32] P. Wardman, Journal of Physical and Chemical Reference Data 18 (1989) 1637–1755.
[33] A.L. Stroyuk, V.M. Granchak, S.Y. Kuchmii, Theoretical and Experimental Chemistry 37 (2001) 174–179.
[34] I. Ilisz, A. Dombi, Applied Catalysis A 180 (1999) 35–45.
[35] S. Tunesi, M. Anderson, Journal of Physical Chemistry 95 (1991) 3399–3405.
[36] C.S. Lu, T-Y. Chiang, Journal of the Chinese Chemical Society 56 (2009) 1118–1127.

[37] M. Sleiman, P. Conchon, C. Ferronato, J.M. Chovelon, Applied Catalysis B: Environmental 71 (2007) 279–290.
[38] A. Piram, R. Faure, H. Chermette, C. Bordes, B. Herbreteau, A. Salvador, Journal of Environmental Analytical Chemistry 92 (2012) 96–109.
[39] R.D. Barreto, K.A. Gray, K. Anders, Water Research 29 (1995) 1243–1248.
[40] C-C. Chen, R-J. Wu, I.-C. Yao, C-S. Lu, Journal of Hazardous Materials 172 (2009) 1021–1032.
[41] K. Nohara, H. Hidaka, E. Pelizzetti, N. Serpone, Journal of Photochemistry and Photobiology A: Chemistry 102 (1997) 265–272.
[42] H. Hidaka, E. Garcia-Lopez, L. Palmisano, N. Serpone, Applied Catalysis B: Environmental 78 (2008) 139–150.